JOURNAL OF SPACECRAFT AND ROCKETS
Vol. 44, No. 3, May–June 2007

# Mars Sample Return: Testing the Last Meter of Rendezvous and Sample Capture

Richard P. Kornfeld*
*Jet Propulsion Laboratory, California Institute of Technology, Pasadena, California 91109*
and
Joe C. Parrish† and Steve Sell‡
*Payload Systems, Inc., Cambridge, Massachusetts 02142*

DOI: 10.2514/1.26098

**One of the key challenges of a future Mars sample return mission is the autonomous capture of an orbiting sample canister, previously lofted from the Martian surface, by an Earth Return Vehicle. To accomplish the capture, the latter spacecraft rendezvous with the sample canister and captures it using a capture cone. Understanding the capture dynamics between the sample canister and capture cone in the zero gravity environment is paramount to designing an effective capture mechanism. Moreover, testing and validating the sample capture event in a zero gravity environment is a crucial, though challenging, element to ensure mission success. Although ground-based simulations and flat-floor facilities are cost-effective, they are lacking the required fidelity. On the other hand, space-based testing opportunities provide a true zero gravity environment, but are prohibitive because of their costs. This paper presents a novel, efficient, and cost-effective way to test and validate the "last-meter" rendezvous and capture event. The testing strategy exploits the zero gravity periods provided by NASA's C-9 parabolic aircraft and a novel free-floating test setup that allows the exploration of various capture conditions in a controlled manner. The testing methodology and test hardware are described, and the results and lessons learned from a weeklong flight test campaign are discussed. The methodology and the conclusions described herein can serve as a pathfinder for the test and validation of other zero gravity capture events including those envisioned for future planetary sample return missions.**

## I. Introduction

OVER the last few years, considerable effort has been invested to define the architecture of a future Mars sample return (MSR) mission. Numerous studies performed by the Jet Propulsion Laboratory (JPL) [1–4], NASA [5], and the industry [6–9] investigated the architectural trades that accompany such a complex mission. Although a definite launch date has not been established, a preferred sample return architecture has emerged and has been documented in [10,11]. The fundamental objective of this mission is to bring back 1/2 kg of sample consisting of rock, regolith, and atmosphere for analysis in terrestrial laboratories. To accomplish this objective, a lander spacecraft equipped with modest mobility, such as a rover, would land on Mars, acquire a sample and stow it in a sample canister, and finally launch the canister from the Martian surface atop a small two- or three-stage solid rocket booster into a low Martian orbit (Fig. 1a). Once in orbit, the orbiting sample canister (OS) would separate from the ascent vehicle and stay in orbit awaiting the arrival of an Earth Return Vehicle.

The size, shape, weight, and makeup of the OS have been subject to extensive debate because it is the pivotal element in the current architecture tying all the other elements together. The OS is currently envisioned to be a sphere with a diameter of approximately 16 cm and a weight of around 5 kg [10,11]. Its outside surface is white to facilitate its detection via cameras on the Earth Return Vehicle. A small uhf beacon transmitter and battery are currently considered as a desirable option.

The Earth Return Vehicle would either be launched in the same opportunity or may arrive at Mars in the next opportunity (i.e., 26 months later). Detection of the OS by the Earth Return Vehicle is envisioned to be via a narrow-angle optical camera, a camera also used to perform optical navigation. Analysis has shown that locating a lost OS from a medium altitude orbit can be achieved within a few days [10]. Alternatively, the uhf beacon could serve as a way to detect the OS orbit. Once the OS orbit is detected, the Earth Return Vehicle would perform a number of maneuvers to navigate into the vicinity of the OS. A wide-angle visible camera is envisioned to be used for close proximity operations, whereas semi-autonomous rendezvous algorithms would guide the Earth Return Vehicle to rendezvous with and finally capture the OS. The Earth Return Vehicle would carry a capture cone to capture and retain the OS. After capture, the OS would be stowed in an Earth Entry Vehicle attached to the Earth Return Vehicle and the spacecraft would then leave Mars to return to Earth. Shortly before arriving at Earth, the Earth Entry Vehicle would be released and the Earth Return Vehicle deflected from the entry trajectory. The Earth Entry Vehicle then enters the atmosphere and could potentially land at the Utah test range, from where the samples would be recovered.

A number of technology validation missions have been flown in recent years or are currently planned in the near future that involve in-space autonomous rendezvous operations. NASA's Demonstration of Autonomous Rendezvous Technology (DART) mission, launched in April 2005, successfully performed an autonomous rendezvous and approach to within approximately 300 ft of the target, but then placed itself in the retirement phase before completing all planned proximity operations, ending the mission prematurely [12]. The Air Force XSS-11 mission, also launched in April 2005, is testing autonomous rendezvous and proximity operations using miniature proximity sensors to inspect other space hardware owned by the United States [13]. Finally, the Defense Advanced Research Projects Agency's Orbital Express, planned for launch in March 2007, aims at demonstrating on-orbit satellite

Received 30 July 2006; revision received 17 December 2006; accepted for publication 27 December 2006. 

*Senior Engineer, Systems and Software Division. Senior Member AIAA.
†President.
‡Senior Systems Engineer.

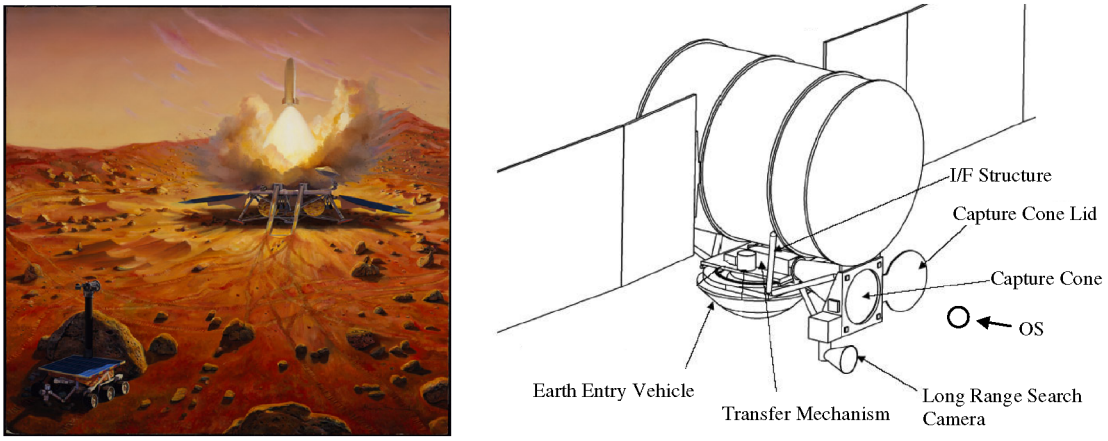


a) b)

**Fig. 1 a) Artist's rendering of ascent booster launch from the surface of Mars; b) Rendezvous and sample capture design concept.**

servicing including fully autonomous rendezvous, submeter range autonomous station-keeping, soft capture, and on-orbit refueling and component replacement as well as other robotic operations [14]. To accomplish these objectives, the mission launches two spacecraft together, the Astro servicing spacecraft and the NextSat serviceable client satellite. In the envisioned mission, Astro uses a robotic arm and grapple fixtures to capture and service the NextSat vehicle.

Although these missions are not directly related to the Mars sample return mission, they do demonstrate and validate various elements of the rendezvous and capture problem, such as rendezvous sensors and rendezvous guidance algorithms that help guide the spacecraft into the vicinity of its target. However, aspects not demonstrated with these missions include the "last-meter problem" of the rendezvous and sample capture, namely autonomously capturing the orbiting sample canister via a capture cone.

In the envisioned MSR mission, the onboard guidance system navigates the Earth Return Vehicle into close vicinity of the orbiting sample canister using a narrow-angle camera. As it approaches the OS with a positive closing rate of a few centimeters per second, its trajectory follows an invisible tunnel that narrows continuously. This is accomplished by continuously decreasing the allowable deadbands, i.e., the allowable excursion from the ideal centerline. As the spacecraft approaches its last meter, the OS has filled the entire camera field of view and no more new measurements are obtained (Fig. 1b). At this point, the spacecraft navigates inertially on a trajectory that should bring the OS well within the circumference of the capture cone. The latter constitutes one of the most challenging aspects of a successful Mars sample return mission, because it is performed autonomously (several light minutes from Earth), requires very tight spacecraft control, and, if not successful, may lead to an uncontrolled collision of the spacecraft and OS. The capture cone needs to be designed and sized to account for errors in the spacecraft's ability to navigate along the desired trajectory (i.e., knowledge and control errors). Moreover, the OS may be spinning or tumbling as a result of the release from the Mars ascent booster upper stage and may have a nonzero incident angle with respect to the capture cone centerline, further complicating the capture dynamics.

To design a capture cone that is robust to both the spacecraft's limited control and knowledge capabilities and the unpredictable OS rotational motion, the complex nature of the capture dynamics and the OS capture cone interactions need to be thoroughly understood. Furthermore, a rigorous test program needs to test and validate the capture cone design under realistic environmental conditions. In particular, for a given capture cone design, the capture "envelope" needs to be characterized because it drives the error requirements levied on the guidance, navigation, and control subsystem. Moreover, whereas ground-based modeling and simulation tools exist to assist in modeling these interactions, these models, too, need to be validated first using real test data.

In this paper, a novel, efficient, and cost-effective way to investigate capture dynamics and to test and validate capture cone designs is presented. It uses NASA's C-9 "weightless wonder" aircraft as a platform to provide short periods of zero gravity [15] and describes a novel test setup that allows the exploration of various capture conditions in a controlled manner.

The paper is organized as follows: Sec. II discusses the cost-benefit trade of the different test and validation options for the last-meter problem. Section III describes the selected C-9 test and validation venue and the necessary hardware and software elements comprising it. In Sec. IV, the actual test campaign and the test results are presented, and the lessons learned and limitations are discussed. Finally, Sec. V summarizes the work and presents conclusions.

## II. Testing and Validating the Last Meter

Key criteria of a good rendezvous and capture test and validation venue include the following:

1) Zero-*g* quality: the quality of the zero-*g* environment (and other applicable environmental effects);
2) Model fidelity: the fidelity of the hardware and software models used to test contact dynamics;
3) Degrees of freedom (DOF): the numbers of DOF usable without constraints;
4) Duration and number of tests: the duration in the relevant environment and the number of tests that can be performed;
5) Failure tolerance: impact and consequences of a failed run and/or test venue element;
6) Availability: availability of test venue;
7) Cost: cost of using test venue.

An alternative approach in assessing the benefit of a test venue is the Technology Readiness Level (TRL) achieved by using this venue [16]. Table 1 provides the description of the TRLs. A TRL of nine implies a technology that is flight proven through successful mission

**Table 1 Technology Readiness Levels (TRL)**

| TRL | Description |
|---|---|
| TRL 1 | basic principles observed and reported |
| TRL 2 | technology concept and/or application formulated |
| TRL 3 | analytical and experimental critical function and/or characteristic proof-of-concept |
| TRL 4 | component and/or breadboard validation in laboratory environment |
| TRL 5 | component and/or breadboard validation in relevant environment |
| TRL 6 | system/subsystem model or prototype demonstration in a relevant environment (ground or space) |
| TRL 7 | system prototype demonstration in a space environment |
| TRL 8 | actual system completed and "flight qualified" through test and demonstration (ground or space) |
| TRL 9 | actual system "flight proven" through successful mission operations |

**Table 2 Cost and benefits for different test venues**

| | Computer sim | 3-DOF flat floor | 6-DOF Flat Floor | Parabolic flight | ISS experiment | On-orbit demo |
|---|---|---|---|---|---|---|
| TRL | 3 | 4–5 | 5 | 6 | 6 | 7 |
| Zero-*g* quality | partial | partial | partial | full | full | full |
| Model fidelity | low | medium | medium | high | high | high |
| DOF | 6 | 3 | 6[a] | 6 | 6 | 6 |
| Duration in relevant environment | unlimited | minutes | minutes | 25 s | hours | hours |
| Number of test runs | 1000s | 100s | 100s | 100s | 10s | 1s |
| Failure tolerance | yes | yes | yes | yes | limited | no |
| Availability | high | high | medium | medium | low | low |
| Cost, $k | 10s | 10s | 100s | 100s | 1000s | 10,000s |

[a]Some limitations to the available DOF imposed by support carriages and structure.

operations. Typically, a system or subsystem test performed in a relevant environment results in a TRL of six and constitutes the prerequisite for being baselined in a flight mission.

A number of possible test venues exist that meet these criteria to a varying degree. They are summarized in Table 2. On the one end of the spectrum, a computer simulation is a venue that is cost-effective and has high availability. However, a simulation is only as good as the models that comprise it. To this end, the simulation needs to be validated first using data from an experiment that provides the highest fidelity possible. Therefore, a computer simulation is not suited as a first step in a validation campaign, but should be used after the mechanics of the impact have been understood and the simulation models validated accordingly.

A higher fidelity test venue is the use of a flat-floor facility. They exercise the capture event using actual physical devices mounted on robotic arms or gantries that simulate the actual trajectory. Both 3-DOF and 6-DOF capabilities exist and the cost to operate them are typically in the tens to hundreds of thousand U.S. dollars. These facilities allow the simulation of the actual spacecraft trajectory and thus are best suited to exercise sensors and proximity guidance algorithms. However, due to the large masses and inertias involved in the gantry system, the venue is not particularly well suited to simulate the low-momentum impact of a sample canister into a capture cone. Moreover, the required suspension systems do not lend themselves well for exercising a capture event, where an unconstrained OS motion is a prerequisite for a meaningful experiment.

A parabolic flight campaign offers a full 6-DOF zero-*g* environment and thus lends itself well to overcome these limitations, albeit for a short time period only. A typical parabola provides zero-*g* conditions for close to 20 s. However, multiple parabolas (typically 40) can be flown in a single flight, thereby offering a zero-*g* environment for a cumulative of a few minutes at a cost comparable to the high-end flat-floor facilities. By using this venue, the technology is demonstrated to a TRL 6, thus readying it to be baselined for a flight mission. The drawback of this option is its susceptibility to atmospheric influences such as wind shear that may lead to imperfect zero-*g* conditions further reducing the amount of time real zero-*g* is attainable. There are only a limited number of government and corporate organizations flying parabolic aircraft, including NASA's C-9 parabolic aircraft, and this venue is thus not as readily available as the other test venues previously discussed.

To obtain zero-*g* conditions for extended periods of time, on-orbit operation is required. A testbed on the International Space Station (ISS) provides undisturbed zero-*g* conditions for long durations of time and allows the repeated execution of unconstrained, 6-DOF capture experiments. Although the test conditions are nearly ideal to meet the objectives of these tests, this venue has a number of significant limitations including the high costs associated with safety and integration of an experiment on the space station, as well as limited availability of manifesting opportunities and on-orbit resources such as crew time.

Finally, to achieve the highest fidelity in simulating on-orbit sample capture, a dedicated free-flyer mission has to be implemented. This offers the opportunity to fully exercise all aspects of a rendezvous and sample capture mission in a relevant environment. Besides the capture dynamics, a slew of other elements can be exercised including sensors and algorithms. Although it offers the ultimate validation and achieves TRL 7, the funding required for a dedicated mission is orders of magnitude higher than for the other venues, the test hardware takes years to develop, and the mission may have a limited lifetime due to finite propellant resources.

Table 2 summarizes the cost and benefits of all test venues discussed in the preceding paragraphs. Based on this analysis, the authors chose the parabolic aircraft because it provided sufficient zero-*g* conditions and the opportunity of true 6-DOF motion to meet the objectives outlined in this paper at the lowest possible cost.

The next section outlines the implications of this choice on the testing methodology, test setup, and instrumentation.

## III. Test Implementation

### A. Testing Methodology

The objectives of a capture cone validation test are twofold. First, it allows the mechanical design engineer to investigate the capture dynamics between the OS simulator[§] and the capture cone, thus providing the insights necessary to make the appropriate design trades. Second, the test enables the characterization of a capture envelope associated with a particular capture cone design. The capture envelope circumscribes the set of capture cone and OS simulator states that lead to a successful capture, including but not limited to quantities such as relative velocity, approach angle, spin rate, and impact points. The envelope is determined by exercising the capture experiment under various capture conditions in a controlled manner. The concept of capture envelope is useful because it ultimately drives the definition of the error requirements levied upon the guidance, navigation, and control subsystem. Moreover, the capture envelope constitutes the framework within which the efficacy of various capture cone designs can be compared against each other.

To conduct an effective test program, the test environment must be well understood and its shortcomings adequately addressed. During parabolic flight, zero-*g* is attained by bringing the aircraft into a 45 deg nose high position and then flying the aircraft "over the top," thereby rotating the aircraft through a 90 deg pitch turn ending in a 45 deg nose low attitude, typically providing zero-*g* time of up to 25 s. This is followed by a "pullout" maneuver lasting about a half minute during which the aircraft experiences 1.8 *g* (i.e., 1.8 times the gravitational acceleration) before it is ready to go into the next parabola. Figure 2a shows a notional aircraft trajectory (altitude) over time during a typical parabola, and Fig. 2b shows a 45 deg nose high position at the onset of the zero-*g* maneuver.

As outlined in the preceding paragraphs, the main limitations of the parabolic flight test venue are the relatively short duration of available zero-*g* time. Moreover, its susceptibility to atmospheric influences such as wind shear may lead to (temporarily) imperfect zero-*g* conditions further reducing the amount of time real zero-*g* is attainable.

To accomplish a sample capture and acquire all the required measurements in the available zero-*g* time, the OS simulator needs to be set up in the desired initial conditions with respect to the capture cone and then captured by the latter before the aircraft emerges from

[§]For the remainder of this paper, the terms OS and OS simulator will be used interchangeably.

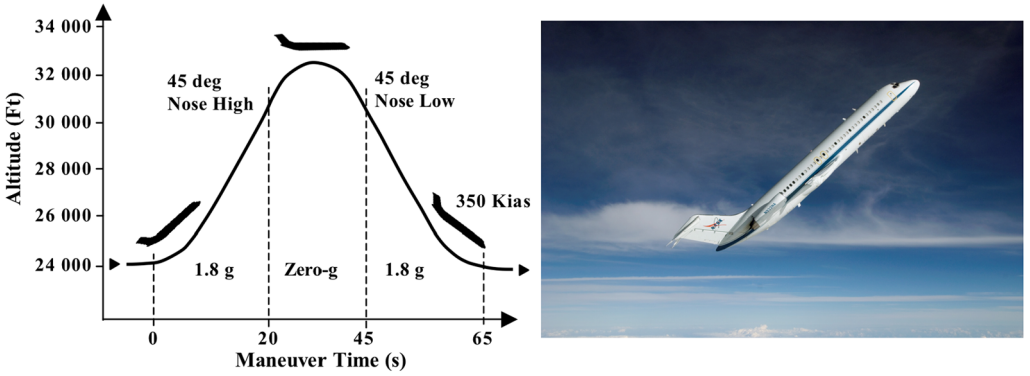


a) b)

**Fig. 2 a) Zero-*g* parabola; b) NASA's C-9 zero-*g* aircraft (source: NASA).**

the zero-*g* portion. To this end, an "OS launcher" is used that propels the OS simulator with the desired velocity and spin rate and with the desired incident angle and offset towards the capture cone. In the MSR mission, the Earth Return Vehicle is maneuvering to capture the OS and the latter is entirely passive. However, the problem is reversible, and in the adopted testing methodology the OS simulator is being maneuvered with respect to the capture cone.

Furthermore, to isolate the experiment as much as possible from atmospheric turbulences as well as the 90 deg aircraft pitch change during the zero-*g* portion, the entire test setup is a free-floater with both the capture cone and launcher mounted to a common frame. The latter is released at the outset of the zero-*g* part and then recaptured toward the onset of gravity. If the aircraft encounters turbulence and/or wind shear during this time period, it will shift the aircraft frame with respect to the free-floater, but does not impart any disturbance accelerations as long as the frame does not hit any of the aircraft interior walls. If, instead, the frame were mounted to the aircraft, all the disturbances (as well as the aircraft pitch rotation) would be measured by the instrumentation.

Similar to the MSR mission, where the OS mass is many times smaller than the spacecraft mass, the OS simulator mass is significantly smaller then the combined capture cone and frame assembly, thereby preserving an accurate representation of the contact dynamics of the OS/capture cone system.

### B. Test Setup Overview

Figure 3 shows the overall test setup. The free-float frame is the overall structural element to which all other hardware elements are attached. Its size is approximately $1.7 \times 1 \times 1$ m. The frame contains a set of rollover bars that protect the test equipment from accidental impact by personnel or when the frame hits the aircraft wall, floor, or ceiling. The capture cone is mounted to the free-float frame via a baseplate that houses most of the instrumentation and avionics. The launcher is shown on the right side of the frame. At the outset of the parabola, it ejects the OS simulator with a preprogramed initial condition. The OS simulator then traverses the distance to the capture cone. As it pierces the capture plane, the lid starts to close thereby capturing and retaining the OS simulator. At the end of the parabola, the flight crew guides the frame to the floor, opens the lid, retrieves the OS simulator, and reloads it into the launcher to be ready for the next parabola. Simultaneously, all the data for this run are downloaded and stored for postflight analysis. The entire test setup is controlled and configured via a laptop computer.

A number of degrees of freedom in setting up a test run allows the effective exploration of the capture envelope. The launcher can be positioned at various distances and angles from the capture cone, allowing varying incident angles as well as different impact locations. Furthermore, the launcher can be programmed to eject the OS at various speeds and spin angles simulating different separation conditions from the booster upper stage. Finally, the capture lid closure rate can be varied to simulate more benign or aggressive capture strategies. Table 3 shows a summary of all the variable test parameters. Major elements of the test setup are explained next in greater detail.

#### 1. *Capture Cone*

The capture cone is shown in Fig. 4a. At the entry plane, its inner diameter is 24 in. and its length is 30 in. Its design is derived from

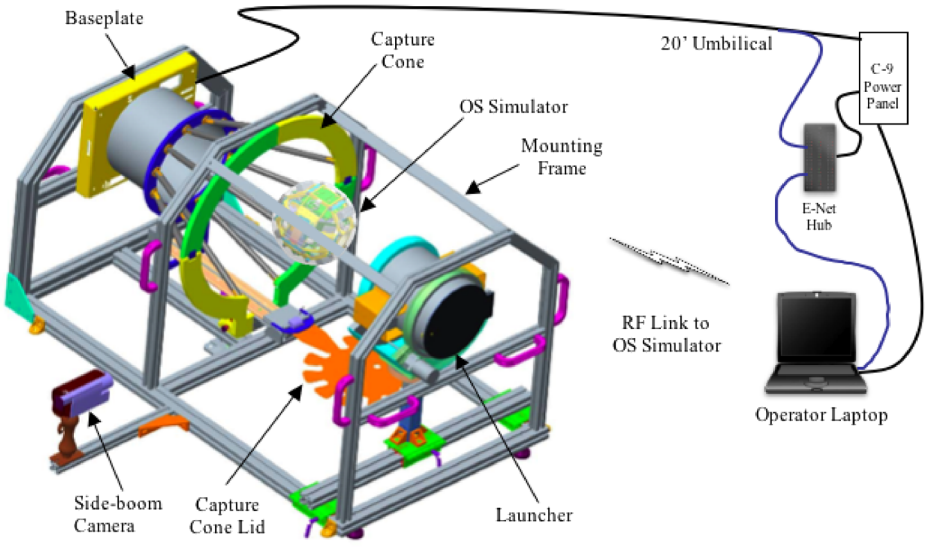


**Fig. 3 Test setup overview.**

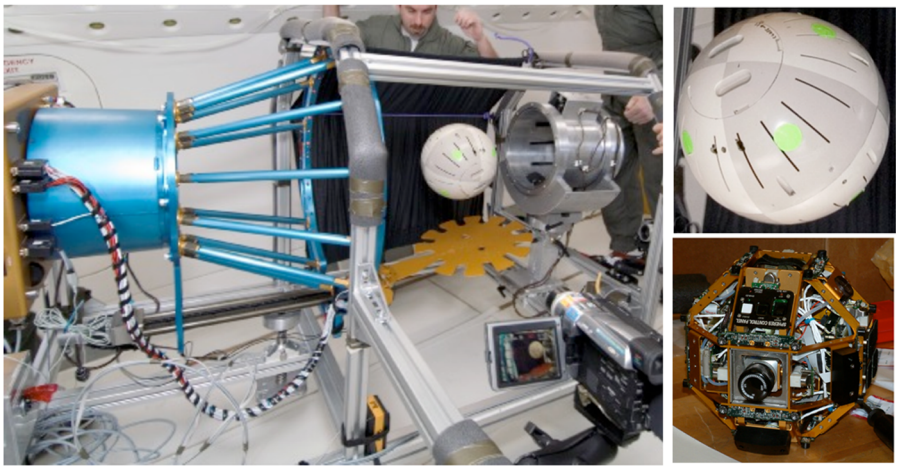

a) b)

**Fig. 4 Test hardware: a) frame, capture cone, and launcher, and b) OS simulator with (top) and without shell (bottom).**

design concepts developed for NASA's (now canceled) 2003/2005 Mars Sample Return mission. It has a single lead screw actuator that, driven by a stepper motor, opens and closes the lid. At the throat of the capture cone is a cylindrical OS receptacle that retains the OS simulator once the lid is fully retracted into the cone. The capture cone rim contains 14 laser beam and detector pairs forming a tight light curtain that defines the entry plane. Once the OS simulator pierces this plane and disrupts at least one of the light beams, the lid closure is triggered. (The number of light beams that need to be interrupted to trigger a lid closure is configurable.) The lid mechanism is spring-loaded to protect it against unintended collisions.

### 2. *Baseplate*

The capture cone is attached to the baseplate via a force-torque sensor that is integrated into the baseplate. The force-torque sensor measures the forces and torques imparted onto the capture cone at the time of the OS simulator impact and is an integral part of the measurements suite. The interface between capture cone and force-torque sensor is modular and allows the attachment of other capture cones should new designs emerge. At the center of the sensor assembly, a boresight video camera is mounted to record the OS simulator motion along the capture cone centerline throughout the test run. The baseplate also houses a computer that controls the capture cone and lid functions as well as collects the sensor information after each run. It communicates with the laptop computer via Ethernet cable, but can also be interfaced with via control buttons and a small liquid crystal display.

### 3. *OS Simulator*

The OS simulator, shown in Fig. 4b, is a fully instrumented, self-contained, 6-DOF, free-flyer satellite, built for operations in pressurized zero-*g* environments. It is based on the existing SPHERES (Synchronized Position, Hold, Engage, and Reorient Experimental Satellites) design [17]. Its spherical form, diameter of 10.25 in. (26 cm), and weight of 4 kg roughly reflects the shape, size, and weight of the envisioned OS, respectively. Its outer shell is a low-cost, polycarbonate spherical shell with a paint pattern conducive to postflight video processing for velocity extraction. It contains an inertial measurement unit (IMU) providing both acceleration and attitude rates, ultrasonic receivers that are part of the positioning system, an onboard computer running attitude and position control algorithms, as well as a cold gas CO2-based propulsion system for attitude and position control. The OS simulator communicates with the laptop computer via wireless RF communications. During each test run, the OS collects onboard gyro and acceleration data. Between runs, the data are downloaded to the laptop. The data are useful in describing the initial state of the OS before impact. For the purposes of the experiment described in this paper, both the propulsion system and the ultrasonic positioning system were disabled.[¶]

**Table 3 Test parameter variation**

| Test parameter | Range |
|---|---|
| OS approach angle | any approach angle that intersects the capture cone |
| OS approach speed | 8–30 cm/s from OS launcher, (>30 cm/s from operator hand-toss) |
| OS impact location | any point on plane of rim |
| OS spin rate | 0–83 deg /s (or greater from operator hand-toss) |
| Capture lid closure rate | lid closure time variable between 5–20 s |

### 4. *Launcher*

The OS launcher is used to accelerate and spin the OS simulator to the desired initial conditions toward the capture cone. Its main structural element is a barrel into which the OS is loaded. On each side of the barrel, a set of two wheels, driven by stepper motors, impart linear and rotational velocity onto the OS, similar to the operating concept of a batting cage baseball pitching machine, although much slower. When the wheels counter-rotate, linear motion is imparted on the OS, whereas a differential rotation imparts an additional rotation component. Depending on the orientation of the barrel, pitch or yaw rotation, or a combination thereof, can be obtained. A third wheel and motor rotate the entire barrel assembly to provide roll rotation. The launcher is controlled via the laptop computer allowing the operator to select spin rates and velocity. The launcher can be positioned at varying positions and orientations (including pan and tilt) with respect to the capture cone allowing the exploration of a large capture envelope.

### 5. *Test Instrumentation*

Besides the force-torque sensor, laser curtain, and boresight camera in the baseplate and the IMU in the OS, there are a number of

[¶]The SPHERES system was originally conceived for use on the ISS. For a capture experiment on the ISS, the onboard guidance and propulsion system could be used to accelerate and spin the OS simulator to the desired initial conditions. However, given the short zero-*g* time interval on the C-9, the available control authority was deemed insufficient to accomplish this task in the available time. Instead, the launcher approach was selected to provide the desired initial conditions. The ultrasonic positioning system relies on five stationary ultrasonic transmitters, mounted rigidly to the aircraft, to enable the SPHERES satellite to triangulate its position. Given the free-flying nature of the entire experiment the absolute position of OS with respect to the airframe was of secondary importance and the positioning system was thus disabled.

**Table 4 Sensor range and resolution**

| Data element | Sensor | Range | Resolution | Rate |
|---|---|---|---|---|
| *OS dynamics* | | | | |
| Approach trajectory | boresight video | 1024 × 768 pixels | <0.2 cm/x-pixel | 15 fps |
| | side-boom video | 720 × 480 pixels | <0.1 cm/y-pixel | 30 fps |
| Approach speed | boresight video | 1024 × 768 pixels | 1 cm/s | 15 fps |
| | side-boom video | 720 × 480 pixels | | 30 fps |
| Approach spin | OS gyros | ±1.0 rad/s | 0.0004 rad/s | 500 Hz |
| *Contact dynamics* | | | | |
| OS impact force | OS accelerometers | ±29.7 *g* | 0.015 *g* | 500 Hz |
| OS impact location | boresight video | 1024 × 768 pixels | <0.2 cm/x-pixel | 15 fps |
| | side-boom video | 720 × 480 pixels | <0.1 cm/y-pixel | 30 fps |
| Cone reaction force | force-torque sensor | ±110 N, *x*–*y* axis | 0.053 N, *x*–*y* axis | 1000 Hz |
| | | ±220 N, *z* axis | 0.106 N, *z* axis | |
| Cone reaction torque | force-torque sensor | ±12.4 N · m | 0.006 N · m | 1000 Hz |
| *Capture event* | | | | |
| OS cone entry | laser curtain | N/A | N/A | 1000 Hz |
| Lid travel | linear displacement sensor | N/A | 7.9E − 5 cm | manually polled |
| Lid closure | microswitch | N/A | N/A | 1000 Hz |
| *Frame acceleration* | | | | |
| Frame acceleration | accelerometer | ±2 *g* | 1.9 m*g* | 1000 Hz |

**Table 5 Summary of test runs**

| | | Release mode | | Test quality | | | | | |
|---|---|---|---|---|---|---|---|---|---|
| Flight No. | Parabolas flown | Launcher | Manual | Test started | Cone contact | Lid trigger | Capture | Clean | No human |
| 1 | 40 | 20 | 10 | 30 | 23 | 20 | 17 | 14 | 11 |
| 2 | 40 | 14 | 9 | 23 | 19 | 21 | 17 | 12 | 3 |
| 3 | 40 | 38 | — | 38 | 32 | 31 | 26 | 20 | 23 |
| 4 | 40 | — | 40 | 40 | 38 | 36 | 31 | 32 | 0 |
| Total | 160 | 72 | 59 | 131 | 112 | 108 | 91 | 78 | 37 |

*Legend*

| | |
|---|---|
| Test started | a test was started during this parabola |
| Cone contact | OS simulator/capture cone contact occurred |
| Lid trigger | laser grid tripped to trigger the lid closure |
| Capture | OS simulator was captured |
| Clean | no frame or OS simulator disturbance event occurred from OS simulator release to first capture cone contact |
| No human | OS simulator was untouched during the run |

additional sensors and video cameras employed. A set of accelerometers is mounted on the frame to measure any disturbance of the free-flyer assembly (e.g., by touching the aircraft wall). A side-looking camera is mounted on a side-boom attached to the frame (shown in Figs. 3 and 4) to provide an orthogonal view of the capture event that enables flight path and velocity reconstruction. Both the boresight and side-boom cameras are synchronized with the rest of the data collection system. Finally, two context cameras are mounted to the aircraft frame at the forward and aft corners of the experiment space within the C-9 aircraft to provide overall context information. Table 4 summarizes the instrumentation setup.

## IV. Test Descriptions and Results

### A. Description and Objectives of Test Campaign

A zero-*g* campaign was conducted in NASA's C-9 zero-*g* aircraft in February 2006. The campaign consisted of four zero-*g* flights, each performing 40 parabolas, for a total of 160 parabolas over the course of a week. On each flight, the 40 parabolas were flown in groups of 10 consecutive parabolas with straight-and-level flight of a few minutes in between the groups to accommodate test setup changes.

As outlined in the preceding paragraphs, the specific test objectives for this campaign included the investigation of the contact dynamics between OS simulator and capture cone, and the initial evaluation of the capture concept and its functionality. In addition, this test served as pathfinder to evaluate the utility of the C-9 parabolic aircraft as a test venue for future capture cone tests and validation efforts.

To meet these objectives, a diverse set of test runs needed to be conducted. To this end, a number of parameters were varied, including the approach speed, spin rates, incident angles, and impact point location. Approach speed and spin rates were adjusted by software command and thus were changed in between parabolas. However, the incident angles and impact locations were set by moving the physical location of the launcher with respect to the capture cone. The latter adjustment had to be made during the break periods between the groups of parabolas. The test matrix was therefore structured with this constraint in mind. In addition, due to launcher control authority issues that surfaced during zero-*g* flight (described next), a number of test runs were conducted with a crew operator "tossing" the OS simulator by hand into the capture cone. Although the initial conditions were not as controllable as with the launcher, this strategy resulted in a diverse set of OS simulator initial conditions that complemented the runs where the launcher was used.

### B. Test Results

Table 5 summarizes the results of the flight campaign. The first two parabolas on the first two flights were used for crew training and acclimatization. Overall, of the 156 planned test runs, 78 yielded useful data. This amounts to 50% of the runs, closely matching preflight predictions that were based on historical data. The reasons for unsuccessful runs are discussed next.

Each of the runs was assessed according to a number of quality criteria, including whether the OS simulator contacted the capture cone, triggered the lid closure, and ultimately was captured by the

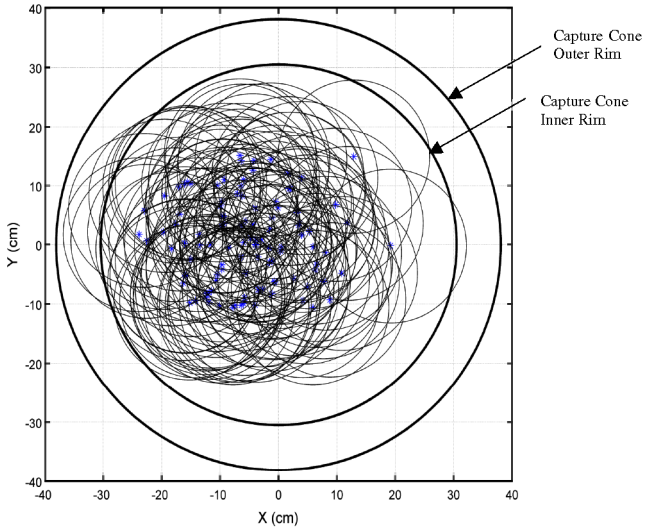


**Fig. 5 OS simulator impact dispersion.**

capture cone. Furthermore, a run was classified as "clean" if neither the OS simulator nor the frame encountered any disturbances from OS release to first contact with the capture cone. The 78 clean runs constitute the useful data set. Finally, in some of the runs, the OS was manually released and/or guided for part of the trajectory or the frame had to be held to avoid hitting the aircraft wall. These interactions did not necessarily invalidate the runs, but instead changed the impact conditions encountered. The number of runs without any human intervention are summarized in the table as well. It is important to note that among the clean runs, there were a number of cases in which the OS simulator escaped the capture cone. These cases are of particular interest to the capture cone designer because they point to the limitations of the current design.

Overall, the efficiency and number of successful runs per flight increased as the weeklong test progressed based on the learning experience of the participating crew. However, atmospheric conditions and resulting pilot performance can affect the overall results significantly, as experienced on flight no. 2. All these factors are explained later in more detail.

Figure 5 shows the off-centerline dispersions of the OS simulator at the time it crossed the capture cone plane. This data was extracted from the boresight camera video based on the time of crossing the laser curtain. Runs where the OS did not cross the capture cone plane (as defined by the laser curtain) are not captured in Fig. 5. As can be seen, a variety of conditions have been exercised including a number of cases where the OS hit part of the capture cone rim. The results from two representative parabolas are discussed next.

### *1. Case Example 1: Flight 1, Parabola 4*

Parabola 4 of flight no. 1 yielded the first successful capture of this campaign. This case was designed to test the overall functionality of the testbed as a system, as well as validate the capture cone concept in its expected nominal operating condition. The launcher was positioned so that the center of the OS simulator was aligned with the capture cone centerline. The test called for an OS simulator velocity of 30 cm/s with zero spin rates on all axes. This run concluded with a successful capture of the OS.

The flight path and capture of the OS simulator are shown in the image sequence in Fig. 6. The screen shots are obtained from both the side-boom and boresight cameras. Note that in the side-looking image sequence, the launcher is on the right-hand side of the frame and the capture cone is on the left. These images also show the laser curtain on the capture cone. Figure 7 shows the data collected for this run, including the measured capture cone force and torque, the times where the laser curtain was pierced, the OS acceleration and spin rate, and the frame acceleration.

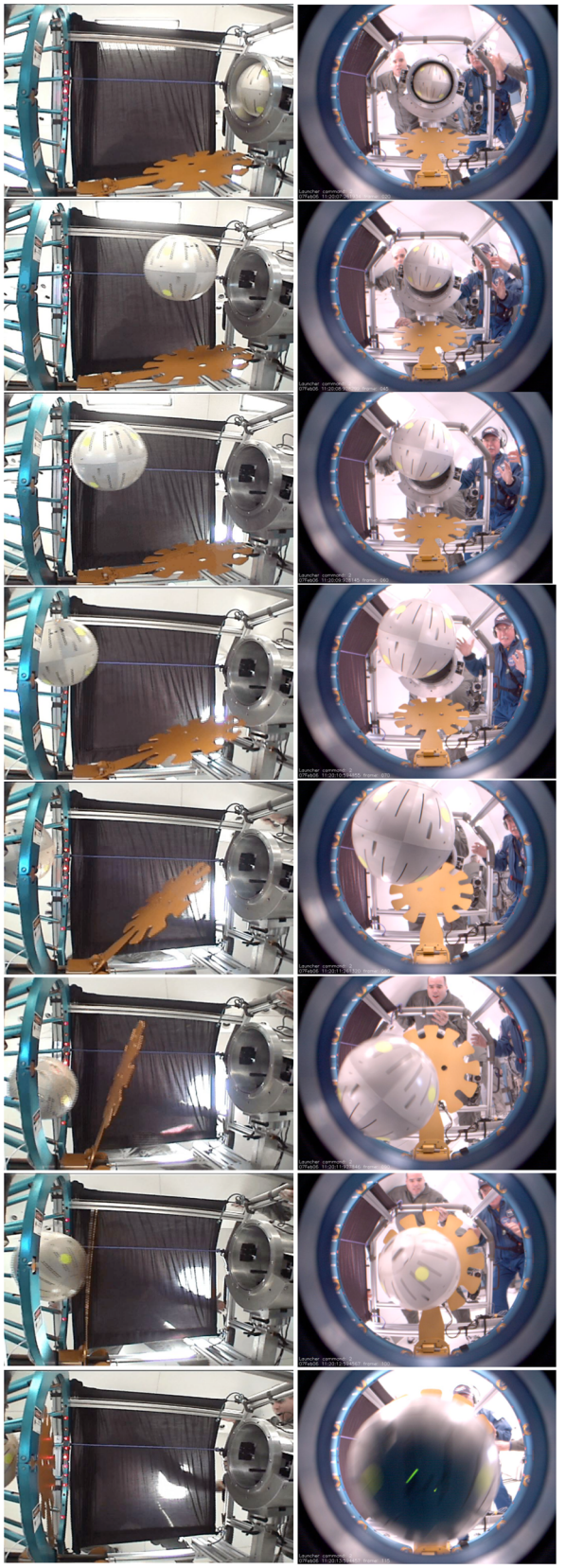

**a) Side camera** **b) Boresight camera**

**Fig. 6 Flight 1, parabola 4 trajectory.**

As visible in Fig. 7, the OS simulator was launched at $t = 1.5$ s, floated towards the capture cone, and pierced the capture plane starting at 4.2 s (the presence of a line in the laser curtain plot indicates that at least one laser was occluded). This triggered the lid motion and, because the capture cone and closing mechanism are

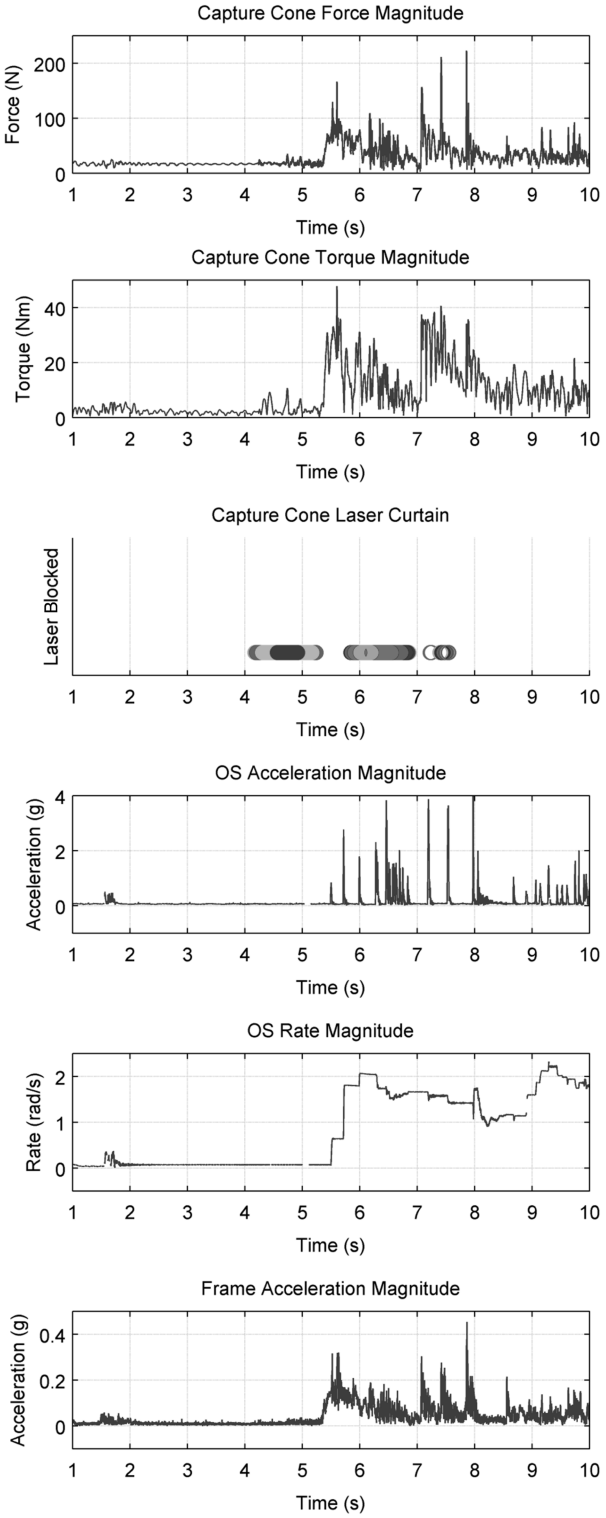


**Fig. 7 Flight 1, parabola 4 data plots.**

structurally connected, this is visible in the force-torque data. First contact with the capture cone occurred approximately 5.5 s into the flight. The OS simulator then bounced around elastically inside the cone and at $t = 5.9$ s pierced the laser curtain a second time on its outbound trajectory (also visible in Fig. 6). The lid then stopped the outbound motion and pushed the OS simulator back into the capture cone for a successful capture. The lid's crossing of the laser curtain is also visible at $t = 7.5$ s. The OS experienced as much as 4 $g$ of acceleration during the capture process and spin rates after contact quickly saturated the rate gyros (nominal range is $\pm 1$ rad/s, however, measurements as high as 1.4 rad/s can be made).

The frame acceleration data helps assess the quality of the run because any disturbance during the free-float time is observable in the data. As can be seen in Fig. 7, there was no disturbance observable (e.g., no contact of the frame with the aircraft or human interaction with the frame) from launch to the initial contact of the OS simulator with the capture cone. Therefore, this run is considered a clean run.

#### 2. *Case Example 2: Flight 1, Parabola 28*

A portion of the planned test matrix was designed to test limit cases of the capture cone system. One such limit case is the "rim shot" where the OS simulator contacts the rim of the capture cone in such a way that it can stop most forward progress of the OS, but still trigger the capture mechanism. This particular test run was intended to be a centerline approach to the capture cone, however, due to some unintentional motion of the testbed just as the OS simulator departed the launcher, the trajectory veered to the side becoming a perfect rim shot. The flight path of the OS simulator is shown in Fig. 8 and the data collected during the run in Fig. 9. Note that in the side-looking image sequence, the launcher is just off the right-hand side of the frame and the capture cone is on the left.

The launcher was positioned so that the center of the OS simulator was aligned with the capture cone centerline and the test called for an OS velocity of 30 cm/s with zero spin rates on all axes. The OS simulator launched at $t = 1.5$ s. During the flight of the OS, there was slight contact of the frame with a human operator. This contact can be seen in the upper right-hand corner of the boresight screen shots in Fig. 8 where a pair of hands can be seen grasping the frame. After launch of the OS, this operator imparted slight motion on the frame to prevent drift from carrying the frame beyond the operational area. Because this contact occurred during the free-flight portion of the OS trajectory, it imparted an apparent drift of the OS simulator relative to the frame and placed the OS on a direct collision course with the rim of the capture cone. At $t = 5.3$ s, the OS simulator pierced the laser curtain and at $t = 5.7$ s the OS simulator impacted the capture cone rim. This event is also captured on the image sequence in Fig. 8 (fifth image from the top). Again, due to the structural connection of the lid closing mechanism and the capture cone, the lid closure is observable in the force-torque data. The OS simulator then bounced off the rim elastically and reversed course with a slight upward velocity. Finally, the lid closed, but failed to capture the OS simulator (its crossing of the laser curtain at $t = 8.5$ s is visible in Fig. 8). The OS simulator experienced as much as 3.6 $g$ of acceleration during the capture process and spin rates after contact quickly saturated the rate gyros.

Close examination of the frame acceleration data reveals a very small disturbance to the frame that caused the OS simulator to deviate its apparent flight (this is not visible in Fig. 9 due to the small scale of the plots). Although originally intended to be a centerline nominal case, this run resulted in an off-nominal case that resulted in an unsuccessful attempt at capturing the OS. It is perhaps from cases such as these that the most useful data can be extracted for future designs.

### C. Discussion and Lessons Learned

This flight campaign studied contact dynamics, evaluated the capture cone concept, and served as a pathfinder for using parabolic flights to test capture events. A discussion of the efficacy of the capture cone, the overall test setup, and the C-9 test venues as well as lessons learned follows next.

#### 1. *Evaluation of Capture Cone and OS Simulator*

Overall, the capture cone appeared suitable to capture the OS simulator. The laser curtain triggered a timely lid closure response and the 1-DOF lid closure mechanism worked as designed by capturing and moving the OS simulator to the cylindrical containment volume at the bottom of the cone. A significant rebound dynamic was observed after the first and subsequent impacts of the OS in the capture cone due to the rigid materials used for both

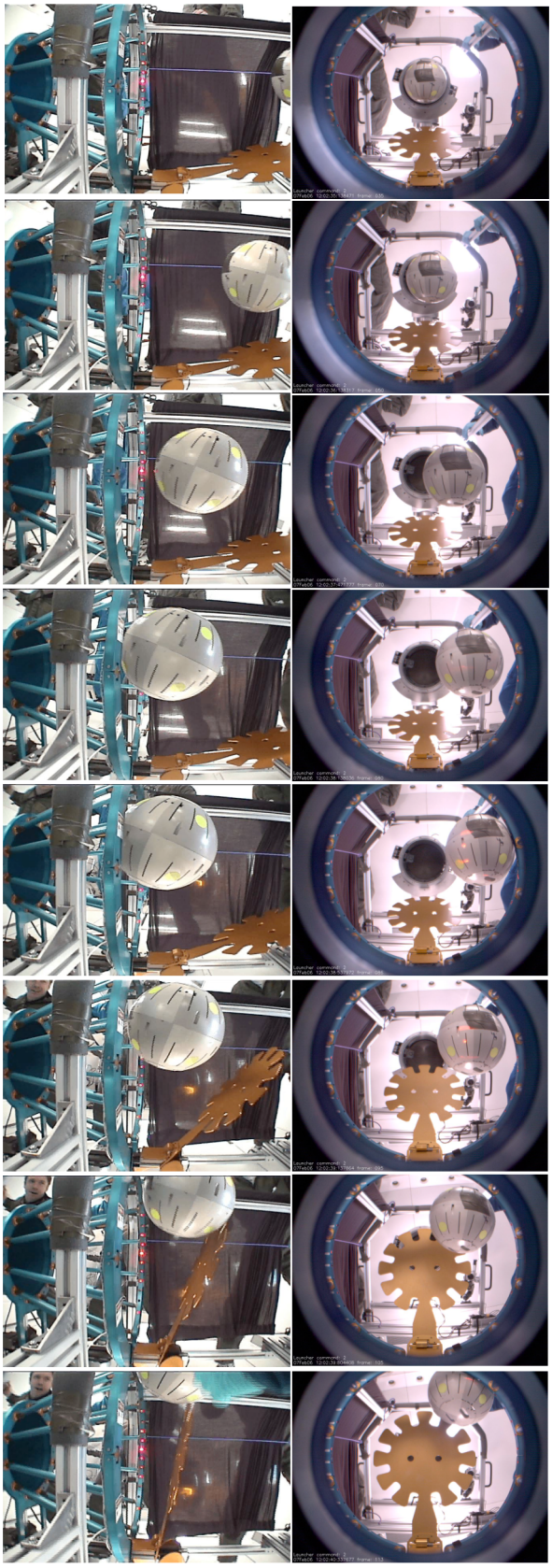

**a) Side camera** **b) Boresight camera**

**Fig. 8 Flight 1, parabola 28 trajectory.**

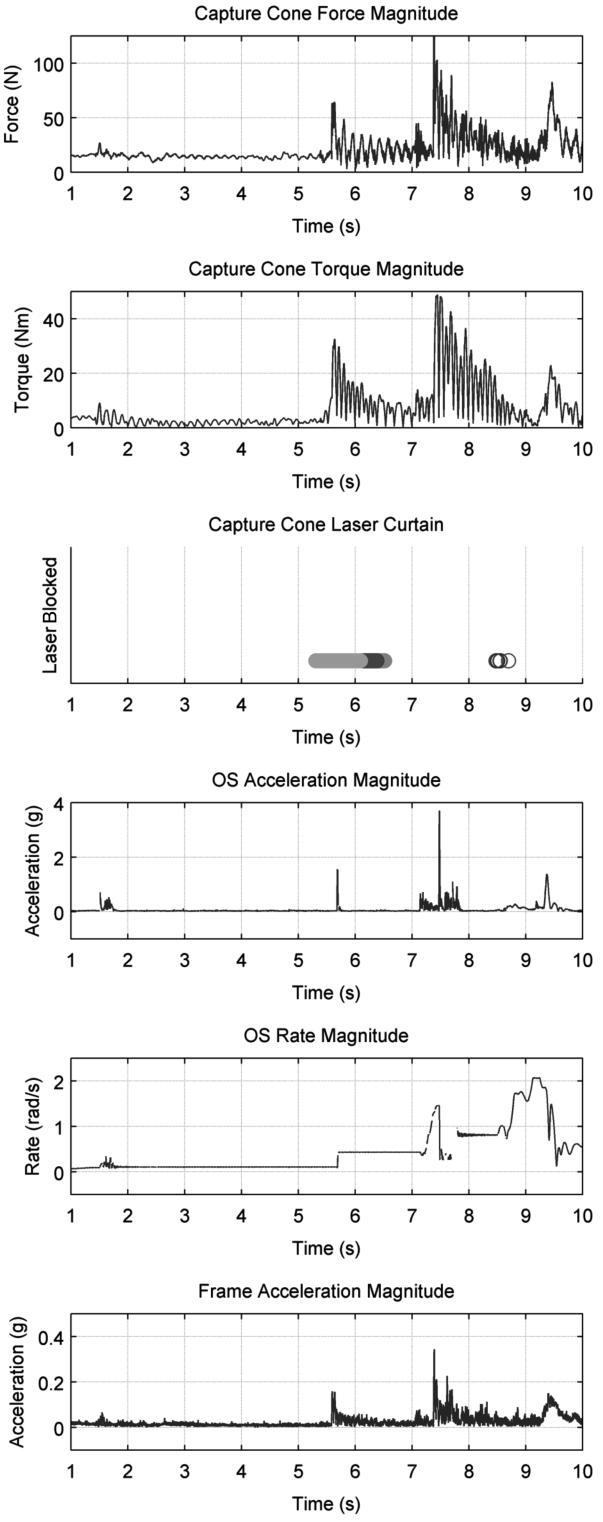


**Fig. 9 Flight 1, parabola 28 data plots.**

the capture cone struts and the OS simulator shell. Future implementations of the capture cone need to address this, for example, by selecting appropriate capture cone materials. For this campaign, the lid mechanism was spring-loaded to protect it against unintended collisions during the experiments. This contributed to a number of runs where the OS simulator escaped again after initial capture. However, this protection feature is not necessary for the MSR flight version.

The OS simulator, although representative in size, shape, and weight to the currently envisioned orbiting sample canister, will continue to be adapted as the latter evolves in the future. For this experiment, a simple spherical geometry and a low-cost polycarbonate shell material was used to simplify contact dynamics analysis. As a final design for a future MSR mission emerges, additional flight campaigns need to be conducted using OS simulators with higher fidelity in geometry and material.

*2. Evaluation of C-9 Test Venue*

The C-9 weightless aircraft performed 160 parabolas in the course of the flight campaign. Fifty percent of the parabolas yielded useful data, matching preflight predictions. During these runs, true zero-*g* was achieved, which offered the opportunity to exercise 6-DOF contact dynamics for short durations. Over the course of the campaign, this allowed the exploration of the operational envelope of the capture mechanism.

Factors contributing to unsuccessful runs were both due to some inherent C-9 venue limitations as well as some test setup deficiencies. Zero-*g* conditions during a number of parabolas were adversely affected by external conditions such as turbulence, wind shear, or minute deviations from the parabolic flight path. Because the airplane was flying through thousands of feet of atmosphere in the course of a parabola, it sometimes encountered wind shear. With the free-floater test frame released at the onset of the parabola in the middle of the crew cabin space, the encounter of wind shear manifested itself by a sudden drift of the free-floater toward the aircraft walls, though in reality the aircraft was being moved laterally with respect to the free-floater. When the free-floater hit an aircraft wall while the OS simulator was in transition, it imparted a disturbance impulse onto the frame, thereby changing the relative velocity and orientation of the frame with respect to the OS simulator. Although not necessarily detrimental to the run, it "randomized" the run from its previously deterministic setup. In a number of cases though, it led to the OS simulator missing the capture cone. Similarly, minute deviations from the parabolic flight path due to pilot control or turbulence, caused the zero-*g* environment to be disturbed or to have a belated onset, thereby significantly shortening the duration of zero-*g* available. With the free-floater released at the perceived onset of zero-*g* in the middle of the crew cabin space, the disturbance or flight path deviation manifested itself by a slow fall of the frame back toward the cabin floor. In most cases, this occurred during the beginning parts of the parabola, when the OS was in transition to the capture cone, thus leading to a failed run. In fact, one of the key challenges for using the C-9 was for the experiment participants to determine when the clean portion of the parabola was reached.

*3. Evaluation of Test Setup*

Tightly coupled with the successful use of the C-9 aircraft was the actual test setup employed for this experiment. As outlined in preceding sections, the test setup was built in a way to accommodate some of the fundamental limitations encountered during the parabolic zero-*g* flight. A common frame was used to isolate the experiment from outside disturbances. In addition, an OS launcher was used to efficiently setup the desired OS simulator initial conditions.

During the flight, the frame served the intended purpose and isolated the experiment from zero-*g* disturbances. The frame also protected the test equipment from accidental impact by personnel or when it hit a wall. However, at the same time, in the presence of disturbances in the zero-*g* environment, the frame contributed to reducing the free-float time because it enlarged the overall envelope of the free-floater, thereby reducing the space for floating. Future test runs need to address this by sizing the frame envelope appropriately.

The launcher was extensively exercised during the campaign and various ejection velocities and spin rates were commanded. Whereas the overall launcher concept was validated, not all desired initial conditions could be obtained under zero-*g* conditions. Straight ejections with or without additional roll spin rate worked as expected, but not yaw and pitch rates and slower ejection velocities due to control authority problems.** To compensate for the inability to obtain all desired initial conditions, the flight crew members reverted to manual tosses of the OS simulator which provided a diverse set of conditions both in velocities and spin rates. For future flights, some simple design modifications are expected to improve launcher performance.

Overall, the sensor suite performed well and all the data were collected. The camera views were adequate to reconstruct the general test environment as well as certain OS simulator state data and experiment events including OS velocity, rim crossing, and contact position. However, the OS simulator rate gyros saturated for some of the hand-toss cases due to the large rotation rates imparted on the OS simulator by the crew member. The frame mounted accelerometers measured all the disturbances encountered by the frame and, together with the context video, allowed the quality assessment of each run. For future flights, additional frame mounted instrumentation would be desirable to measure the disturbance-induced frame rotation.

**All the envisioned operating velocities and spin rates had been successfully tested preflight under 1-*g* conditions.

## V. Summary and Conclusions

This paper describes a novel, efficient, and cost-effective way to test and validate the last-meter rendezvous problem. It relies on NASA's C-9 parabolic aircraft as a platform to provide short periods of zero gravity. A novel test setup allows the exploration of various capture conditions in a controlled manner and enables the efficient evaluation of capture cone designs. The flight campaign described herein served as a pathfinder for investigating capture dynamics and capture cone efficacy. A total of 160 parabolas were flown, half of which resulted in successful test runs, matching preflight predictions. The overall test setup performed as expected, though a number of shortcomings have been identified.

Parabolic flight offers a feasible simulation environment to study OS contact dynamics. It offers true zero-*g*, 6-DOF contact conditions for up to 20–25 s, although zero-*g* durations of 5–10 s are more typical for the test setup used in this campaign. The test venue is cost-effective by orders of magnitude in comparison to space flight (ISS or free-flyer in Earth or Mars orbit) and allows repeated tests with marginal additional cost.

At the same time, the capabilities and limitations of the test hardware and the C-9 parabolic aircraft test venue must be understood and addressed. The original philosophy going into these tests was based on the desire to explore the test space in a deterministic manner by fully controlling the OS simulator state at impact (i.e., full state knowledge and control). To increase the likelihood of achieving full control, the tests need to be of sufficient short duration or the free-float time needs to be extended by reducing the envelope of the test setup. Alternatively, a more probabilistic approach can be adopted in which the aircraft disturbances are used to randomize the experiment set. To this end, manual tosses, as well aircraft disturbances, are used to obtain a diverse set of initial and impact conditions. The key to make the latter approach successful is the availability of full state knowledge of both the OS simulator and the free-float frame by measuring their full 6-DOF dynamics.

As future Mars sample return OS designs emerge, additional testing will be necessary. The testing methodology outlined in this paper can significantly contribute to the efficient and cost-effective execution of these test and validation efforts.

## Acknowledgments

The authors would like to thank Tom Rivellini, Don Bickler, Sean Haggart, Ben Thoma, and Mike Shafer, all of the Jet Propulsion Laboratory Mechanical Systems Division, for their contributions to the design of the capture cone and overall experiment concept, and Richard Mattingly, Mars Sample Return study lead, and Michael Wilson, of the Jet Propulsion Laboratory Autonomous Systems Division, for their systems engineering support. The authors would like acknowledge Edmund Kong and David Miller, both of the Massachusetts Institute of Technology Space Systems Laboratory, for their contributions to the experiment and postprocessing software, and Edison Guerra, Cecil van der Merwe, and John Merk, all of Payload Systems, Inc., for the electrical and mechanical integration of the experiment hardware. The authors would like to thank John Yaniec and Dominic Del Rosso, both of the NASA Johnson Space Center Reduced Gravity Program, for supporting the test campaign on the C-9 parabolic aircraft. The authors would like

acknowledge the support of Samad Hayati, Mars Exploration Directorate Chief Technologist, Suraphol Udomkesmalee, of the Jet Propulsion Laboratory Autonomous Systems Division, and James Jordan, Mars Advanced Studies and Pre-Projects Office Manager, for their continued support and encouragement throughout the duration of this experiment.

This research was carried out at the Jet Propulsion Laboratory, California Institute of Technology, under a contract with NASA. Reference herein to any specific commercial product, process, or service by trade name, trademark, manufacturer, or otherwise, does not constitute or imply its endorsement by the U.S. Government or the Jet Propulsion Laboratory, California Institute of Technology.

## References

[1] Mattingly, R., Matousek, S., and Jordan, F., "Continuing Evolution of Mars Sample Return," *2004 IEEE Aerospace Conference Proceedings*, Vol. 1, IEEE Publications, Piscataway, NJ, 2004, pp. 477–492.

[2] Mattingly, R., Matousek, S., and Jordan, F., "Mars Sample Return, Updated to a Groundbreaking Approach," *2003 IEEE Aerospace Conference Proceedings*, Vol. 2, IEEE Publications, Piscataway, NJ, 2003, pp. 745–758.

[3] Mattingly, R., Matousek, S., and Gershman, R., "Mars Sample Return: Studies for a Fresh Look," *2002 IEEE Aerospace Conference Proceedings*, Vol. 2, IEEE Publications, Piscataway, NJ, 2002, pp. 509–515.

[4] Oberto, R., "Mars Sample Return, a Concept Point Design by Team-X (JPL's Advanced Project Design Team)," *2002 IEEE Aerospace Conference Proceedings*, Vol. 2, IEEE Publications, Piscataway, NJ, 2002, pp. 559–573.

[5] Stephenson, D., "Mars Ascent Vehicle: Concept Development," *38th AIAA/ASME/SAE/ASEE Joint Propulsion Conference and Exhibit, Indianapolis, IN*, AIAA Paper 2002-4318, 2002.

[6] Evanyo, J. A., Delamere, A., Gulick, D., Horsley, B., Fischer, C., Mann, D., Miller, K., Mitchell, S., Svitek, T., Padavano, J., Whittaker, R., Uphoff, C., Helleckson, B., Loucks, M., Boynton, J., and Mungas, G., "Mars Sample Return, a Robust Mission Approach for 'Getting the Right Sample'," *2002 IEEE Aerospace Conference Proceedings*, Vol. 2, IEEE Publications, Piscataway, NJ, 2002, pp. 522–528.

[7] Sherwood, B., Pearson, D., Smith, D. B., Greeley, R., Whittaker, W., Woodcock, G., Barton, G., and Siegfried, W., "Mars Sample Return: Architecture and Mission Design," *2002 IEEE Aerospace Conference Proceedings*, Vol. 2, IEEE Publications, Piscataway, NJ, 2002, pp. 536–542.

[8] Sutter, B., and McGee, M., "Mars Sample Return: The Design of Low Risk Architectures," *2002 IEEE Aerospace Conference Proceedings*, Vol. 2, IEEE Publications, Piscataway, NJ, 2002, pp. 548–554.

[9] Balmanno, W. F., Whiddon, W. B., and Anderson, R. L., "Mars Sample Return Mission Studies Leading to a Reduced-Risk Dual-Lander Mission Using Solar Electric Propulsion," *2002 IEEE Aerospace Conference Proceedings*, Vol. 2, IEEE Publications, Piscataway, NJ, 2002, pp. 558–564.

[10] Mattingly, R., Hayati, S., and Udomkesmalee, G., "Technology Development Plans for the Mars Sample Return Mission," *2005 IEEE Aerospace Conference Proceedings*, IEEE Publications, Piscataway, NJ, 2005, pp. 982–995.

[11] Mattingly, R. L., "Many Faces of the Mars Sample Return Mission Architecture," *Advances in the Astronautical Sciences*, Vol. 121, American Astronautical Society Paper 05-066, 2005, pp. 325–338.

[12] Morring, F., "Target Practice," *Aviation Week and Space Technology*, Vol. 164, No. 21, 2006, pp. 37–38.

[13] Dornheim, M., "Rendezvous Trials," *Aviation Week and Space Technology*, Vol. 162, No. 16, 2005, pp. 35–36.

[14] Dornheim, M., "Express Service," *Aviation Week and Space Technology*, Vol. 164, No. 23, 2006, pp. 46–50.

[15] Yaniec, J. S., and Rosso, D. D., "JSC Reduced Gravity Program User's Guide," NASA AOD 33899 Rev A PCN 1, Aug. 2005.

[16] Mankins, J. C., "Approaches to Strategic Research and Technology (R&T) Analysis and Road Mapping," *52nd International Astronautical Congress, Toulouse, France*, International Astronautical Federation Paper 01-U202, Oct. 2001.

[17] Saenz-Otero, A., Chen, A., Miller, D. W., and Hilstad, M., "SPHERES: Development of an ISS Laboratory for Formation Flight and Docking Research," *2002 IEEE Aerospace Conference Proceedings*, Vol. 1, IEEE Publications, Piscataway, NJ, 2002, pp. 59–73.

J. Korte
*Associate Editor*